

## Curriculum Vitale

Name: Daniel Thomas Fontaine

Contact Information: dfontaine@umaryland.edu

Degree and Date to be Conferred: M.S., 2017

Collegiate Institutions Attended:

Virginia Polytechnic Institute and State University, Blacksburg, VA  
August 2009 – May 2013  
B.S. Biochemistry, Microbiology/Immunology, 2013  
Minor: Chemistry

University of Maryland, Baltimore, Baltimore MD  
August 2015 – May 2017  
M.S. Cellular and Molecular Biomedical Science

Major: Cellular and Molecular Biomedical Science

Positions Held:

Clinical Research Associate, *Blanchette Rockefeller Neuroscience Institute*  
Rockville, MD, 2013 – 2015

Special Awards:

Poster Presentation:  
American Association for Cancer Research Annual Meeting,  
April 2017, Washington D.C.  
*Enhancing the therapeutic effects of PARP inhibitors in combination with DNA methyltransferase inhibitors, using low doses of ionizing radiation in non-small cell lung cancer.*

## **Abstract**

Enhancing the Therapeutic Effects of PARP Inhibitors in Combination with DNA Methyltransferase Inhibitors Using Fractionated Low Doses of Ionizing Radiation in Non-Small Cell Lung Cancers.

Daniel Fontaine, Masters of Science, 2017

Dissertation Directed by: Feyruz V. Rassool, Ph.D., Associate Professor, Department of Radiation Oncology

Non-small cell lung cancer (NSCLC) is the leading cause of cancer-related deaths in the US. Treatment relies on radiation therapy and chemotherapeutics when surgery is not an option. These treatments have significant negative effects on long-term survival. Previous work in the Rassool laboratory found that combining low, non-cytotoxic doses of poly(ADP-ribose) polymerase (PARP) and DNA-methyltransferase (DNMT) inhibitors increased cytotoxicity in AML and breast cancers. This work highlighted the trapping of both proteins at DNA damage sites, creating cytotoxic double strand breaks (DSBs). We examined this combination in NSCLC and whether low doses of ionizing radiation (IR) would increase treatment efficacy. Introduction of IR with this combination, resulted in decreased cell clonogenicity and increased DSB formation. In vivo testing of this combination with IR showed significantly reduced tumor growth and extended survival rates. This suggests that PARP and DNMT inhibitors in combination with IR could be a novel therapeutic for NSCLC.

Enhancing the Therapeutic Effects of PARP Inhibitors in Combination with DNA  
Methyltransferase Inhibitors Using Fractionated Low Doses of Ionizing Radiation in  
Non-Small Cell Lung Cancers.

by  
Daniel Thomas Fontaine

Thesis submitted to the Faculty of the Graduate School of the  
University of Maryland, Baltimore in partial fulfillment  
of the requirements for the degree of  
Masters of Science  
2017

## Acknowledgments

I would like to thank Dr. Rassool for the opportunity to work and learn in her lab over the past 2 years. This has been a huge step in my growth as a scientist and I could not have done it without her expertise and guidance.

I would like to thank the members of the Rassool Laboratory past and present, especially Nidal Muvarak, Lena McLaughlin, Lora Stojanovic, Christopher Biondi, Bryan Pelkey, Aksinija Shamah, and Pratik Nagaria. Their advice and suggestions have been more than helpful in bringing this project to where it is now. You have all made learning and using new laboratory techniques so much easier, and I don't know if this all could have been done without you.

I would also like to thank my thesis committee members, Dr. Feyruz Rassool, Dr. Javed Mahmood, Dr. Rena Lapidus, and Dr. Antonino Passaniti for their tireless aid and guidance towards the final completion of this project.

Lastly, I would like to thank my family for their unending support throughout my time at UMB. You have made trying times so much easier and given me a place to get away when I needed to clear my head. I can't thank you enough for all that you have provided for me.

## Table of Contents

Chapter	Page
ACKNOWLEDGMENTS.....	iii
I. INTRODUCTION.....	1
A. Non-Small Cell Lung Cancer.....	1
B. Standard Radiation-Based Therapies.....	4
C. NSCLC Therapeutic Strategies.....	7
D. PARP1 and PARP Inhibition.....	9
E. DNMT1 and DNMT Inhibition.....	14
F. Combination in NSCLC with Low-Dose Ionizing Radiation.....	16
II. RADIATION ENHANCES THERAPEUTIC EFFECT OF PARPi AND DNMTi COMBINATION IN NSCLC.....	19
A. Inhibitor Combination Effect on Cell Clonogenicity.....	20
B. Co-treatment with IR Decreases Clonogenicity of PARPi and DNMTi Combination.....	22
C. Synergistic Relationship Between PARPi and DNMTi Combination.....	24
D. Molecular Analyses of Therapeutic Effects.....	26
III. CONCURRENT RADIATION THERAPY INCREASES IN VIVO EFFICACY OF INHIBITOR COMBINATION IN NSCLC.....	29
IV. DISCUSSION.....	34
V. MATERIALS AND METHODS.....	39
VI. REFERENCES.....	43

## List of Tables

<u>Table</u>	<u>Page</u>
1. Treatment Groups for <i>in vivo</i> NSCLC Studies.....	30

## List of Figures

<u>Figure</u>	<u>Page</u>
1. PARP Inhibition During BER and SSB Repair.....	11
2. Co-Treatment with DNMT and PARP Inhibitors.....	17
3. Combination Treatment with Tal and AZA Reduces Survival and Clonogenicity in NSCLC Cell Lines.....	20
4. Introduction of IR Further Reduces Clonogenicity in NSCLC.....	22
5. MTS Analysis of PARPi and DNMTi Combination Treatment.....	23
6. Co-Treatment with PARPi and DNMTi Show Synergistic Relationship.....	24
7. IF-Stained $\gamma$ H2AX Foci in RA549 NSCLC Cells.....	25
8. PARPi and DNMTi Treatment in Combination with Single Dose IR Increases $\gamma$ H2AX Foci Formation and Extends Retention Time.....	27
9. Addition of Single Dose IR Failed to Alter Efficacy of PARPi and DNMTi Combination Treatment.....	31
10. Fractionated IR in Combination with PARPi and DNMTi Delayed Tumor Growth.....	33

## **Chapter 1: Introduction**

### *Non-Small Cell Lung Cancer*

The annual Facts and Figures Report for 2017, released by the American Cancer Society, estimates that there will be a combined 240,000 newly diagnosed cases of lung and bronchial cancer spread between men and women of all ages. ACS reports have shown that the number of lung cancer-related deaths has fallen somewhat consistently over the past 10-20 years. However, estimates for 2017 predict that lung cancer will still be responsible for 27% and 25% of all cancer-related deaths in men and women in 2017, respectively; which is greater than the next three most prevalent cancer types (breast, colon, and prostate) combined (Siegel, 2017). Staging of NSCLC patients is largely dependent upon three individual measurements: tumor size (T), local lymph node association (N), and metastasis (M) into adjacent lung or secondary locations throughout the body. This system, commonly referred to as TNM, is used to measure the development of the tumor. As the three measurements (T, N, or M) increase in value, the tumor is considered more advanced, with higher rates of secondary metastasis and lower patient survival rates. The metastatic spread of NSCLC tumors most commonly originates from the primary tumor into local lymph nodes, usually identified as stage I/II, early staged, but remain local (Hopwood, 1995). This results in N-value of the TNM scale moving from 0 to 1. As the primary and surrounding minor tumors progress, they create a larger tumor body around the site of origin. Tumors of this size are considered stage III, locally advanced tumors, and can easily begin to spread to more distant lymph nodes within the same lung. Stage III NSCLC can be characterized by an increased number of tumorigenic cells moving throughout the lymphatic system of both lungs.

These migrating cells can eventually settle in other regions of the lung, including the adjacent lung, resulting in the creation of a secondary tumor in which the patient is considered stage IV (Hopwood, 1995). Patients in stage IV will have higher reported measurements for the T and N values, and will begin to see increased values for M as metastatic tumors begin to form in other regions of the body.

Lung cancers have been divided into 6 individual histological classifications that can be grouped into one of two major types. Non-small cell lung cancer (NSCLC) is the larger of the two main lung cancer groups, comprised of 4 of the 6 classifications, including adenocarcinomas, large cell, squamous cell, adenosquamous, and sarcomatoid carcinomas. The NSCLC groups, as a whole, make up for 80-85% of all lung cancer occurrences (Woodard, 2016). Each classification is differentiated primarily on the site of origin within the lung; more specifically, the structural component of the lung from which the tumor originated. Tumors usually develop from one of two main regions of the lung. Certain tumor types are derived from the peripheral epithelial cells that create the outer lining of the lung, which are commonly classified as adenocarcinoma or large cell carcinomas. Other tumor types, like squamous cell carcinomas, are derived from more central structural components of the lung, including the main bronchi that lead into branching structure of the airways within each lobe. Other more minor classifications are primarily combinations of multiple cell types originating from regions that connect different structural components (Kenfield, 2008).

Despite the various locations of tumor origin, there is minimal variance in the unique molecular features between classification groups. This creates a relatively uniform set of molecular characteristics/markers that can be used to describe almost all

classifications of NSCLC tumors. Many of these markers focus on initiation or inhibition of cell growth and tumor progression, while others work towards the creation of tumor-supporting environments or drive tumor development and metastasis. Point and missense mutations seen in *RAS* and *P53*, genes/gene products, are strongly associated with exposure to tobacco smoke and therefore commonly identified in NSCLC tumors. Point mutations in *RAS*, with *KRAS* contributing to 90% of all *RAS* mutations in all adenocarcinoma patients, have widespread effects on the regulation of cell growth, proliferation, and apoptosis. *RAS* mutations have been identified as a poor prognostic marker for overall survival, and have been linked as a negative marker for sensitivity to anti-EGFR targeted therapies, like erlotinib and gefitinib. (Rose-James, 2012) Missense and point mutations within the *P53* gene results in drastic changes in cell cycle progression, p53-regulated DNA damage repair, apoptosis induction, and countless other tumor-suppressive pathways. With such a wide-spanning range of actions, mutation rates in NSCLC patients can vary significantly based on the pathways effected by the specific mutation. For example, changes in *P53* expression predicts sensitivity to platinum-based chemotherapy, while certain mutations in p53 activity were found to predict resistance to these same treatments. Overall though, most mutations in *P53*/p53 expression and activity were correlated with unfavorable outcomes in adenocarcinomas and squamous cell carcinomas (Rose-James, 2012). Other markers have been more closely linked with tumor progression and metastasis, including vascular endothelial growth factor (VEGF) and CD44 (Rose-James, 2012, D'Amico, 1999). VEGF signal protein that is released by cells in order to recruit endothelial cells and stimulate angiogenesis. CD44 is a cell surface glycoprotein that controls cell to cell adhesion and mitigates cell migration.

Together, mutations in both of these proteins can induce the creation of blood vessels to further stimulate tumor growth (VEGF), and in turn favor the release of tumorigenic cells into the systemic circulation (CD44) (D'Amico, 1999). Both of these markers have been linked with increased rates of recurrence in early staged NSCLC patients, and in turn linked with poor outcomes in later staged patients.

### *Standard Radiation-Based Therapies*

Radiation-based therapies have been a standard of care and one of the most common treatment options for solid tumors, preeminently in internal tumors that would otherwise require overly-invasive surgeries. Radiation has also been used as an adjuvant therapies to tumor resection and chemotherapy in an effort to eliminate any remaining tumorigenic cells that may otherwise cause patient relapse. In lung cancer, radiation in combination with other chemotherapeutics has been a favored tool for tumor removal, mainly due to the difficulty of surgically removing masses from the lung without hampering lung function (Pisters, 2007). Using these combinations generally gives more favorable outcomes in patients in non-early stages of lung cancer.

Therapies utilizing exposure to ionizing radiation (IR) are designed to induce DNA damage in highly proliferative cells and tissues that will result in cytotoxic outcomes during proliferation. Ionizing radiation, by definition, is a particle or wave released with enough energy to remove electrons from the orbit of an atom as it passes through said atom, resulting in the creation of an ion. These particles are used clinically to exert substantial amounts of energy on a targeted region of the body, mainly the tumor

mass, in order to induce damage to genetic material. Exposure to radiation can act on a cell in one of two ways. The first is through direct interaction with the genetic material. As high-energy particles pass through the cell, they can interact or basically collide with the DNA resulting in a large transfer of energy. As with any high-energy collision, this interaction between the particle and the DNA releases energy and results in the creation of a single or double strand break (Santivasi, 2014). The second mode of action is through the creation of reactive oxygen species (ROS) that are a result of particle interactions with water. As ionizing radiation passes through molecules of water, it actuates the release of electrons from the atom, creating ions, a process called radiolysis. ROS are chemically reactive intermediates that will attempt to oxidize any molecule/compound they come into contact with. These species often react with the DNA confined to the nucleus, creating non-bulky and bulky lesions as well as abasic sites as the ROS oxidize the nitrogenous bases. These lesions and abasic sites, if not repaired properly will culminate into single and double strand breaks as the cell moves through DNA replication (Santivasi, 2014).

However, as with any form of cancer therapeutic, the most apparent issue lies in our ability to limit damage to non-tumorigenic tissue. While IV and orally administered chemotherapeutics spread DNA destabilizing and antiproliferative agents throughout the body, radiation therapies require passing significant amounts of energy through an organ and otherwise healthy tissues. Patients that undergo radiation therapy, often experience decreased or loss of lung function due to lung tissues become scarred and inflamed. Studies into NSCLC patients have exhibited a dismal 17% survival rate over the first 5 years after remission (Siegel, 2016). These poor outcomes are attributed to radiation-

linked diseases like pulmonary fibrosis (excessive scar tissue) and radiation pneumonitis (tissue inflammation within airways) that are common occurrences after high-dose radiation therapy (Rodrigues, 2004). Methods of limiting the required doses of radiation while maintaining effectiveness have been difficult to obtain. The widely-established method of radiation treatment in cancer patients has been the creation of dosing schemes that divide a single large dose into a series of smaller doses given over a longer length of time. This dosing scheme is referred to as fractionated dosing. Fractionated dosing is designed to lower the doses that the body is exposed to at a single time while also giving the body, and more specifically non-highly proliferative tissues, more time to repair damage and recover from sub-lethal doses between each exposure. Normal dosing schemes for patients with unresectable lung cancer usually require a total dose of 80Gy which is normally spread over a period of 8 weeks (10Gy/week). Fractionated dosing of this treatment scheme would divide the 10Gy/week rate into 2Gy once a day over 5 days with 2 days of rest in between each set (Ramroth, 2016). This compared to a single 10Gy dose or two 5Gy doses per week will result in far less off-target toxicity with only slight decreases effectiveness (Kong, 2014). Fractionated dosing has greatly increased treatment survivability, but has not had a significant effect on treatment success (Siegel, 2017). Hence the need to develop new combinations that can act upon the effects of radiation in an attempt to increase efficacy, while maintaining safety by allowing clinicians to lower exposure rates.

## *NSCLC Therapeutic Strategies*

While the rate of lung cancer-related deaths is slowly falling, NSCLC still remains a very prevalent, high-risk disease that will require the development of more effective therapy options. Therapeutics for lung cancer, as with many other forms of cancer, tend to be limited by our ability to clinically identify and diagnose tumorigenic growth. Identifying problematic growths early, generally results in increasingly favorable outcomes. However, when solid tumors begin internally, as in the case with lung cancer, they can often be overlooked until the patient notices the physical effects like difficulty breathing, loss of appetite, coughing, and shortness of breath (Hopwood, 1995). These effects may only present themselves in the latter stages of tumorigenesis, which begins to limit our ability to treat them safely. This is the case with NSCLC, where early staged tumors (stage I and II) remain relatively small and confined to a solitary location, but their small size may have a negligible effect on overall lung function (Hopwood, 1995). Common therapeutic strategies usually begin with tumor resection combined with adjuvant radiation and/or chemotherapy, similar to that of most breast cancers. However, depending on tumor size in more advanced patients, significant tissue loss can impair the lung to a point of complete loss of functionality. Consequently, later-staged diagnosis of NSCLC patients can push tumors beyond the limits of resection where clinicians must resort to more potent and therefore harmful treatments that often result in toxic effects in normal tissue (Palma, 2013). These strategies typically rely on platinum-based chemotherapeutics (cisplatin and carboplatin) or high dose radiation therapy that all have the capability of producing off-target effects on highly-proliferative

tissues and the induction of pulmonary fibrosis (excessive build-up of scar tissue in the lung) (Lynch, 2005, Kim 2005).

This has led to a large-scale shift in focus to novel targeted therapeutics that can be aimed against specific genetic and physiological characteristics of tumor cells. New drug products that have come from this new direction have included angiogenesis/VEGF, EGFR, and TKI inhibitors that are all focused towards the cellular requirements for tumor growth, while limiting the possibility of off-target effects (Nguyen, 2012, Paez, 2004). Unfortunately, there has been difficulty in the identification of effective targets in some NSCLC subtypes, mainly within the adenocarcinoma subtype that makes up approximately 40-50% of all NSCLC cases. Only 15-20% of adenocarcinomas harbor genetic abnormalities that can be used as targets for therapeutics; none of which have yet led to significant increases in favorable outcomes (Nguyen, 2012). However, studies have begun to point out certain epigenetic alterations that have been strongly associated with tumorigenesis, and have become possible targets for novel targeted therapies. Given that radiation is still a standard therapeutic modality, efforts have been made to treat NSCLC with drugs that can sensitize cells to lower doses of radiation, thus sparing more normal tissue (Eberhardt, 2006). In the next sections, we will focus on the role of two drugs that have been shown to be radiosensitizers, PARP inhibitors and DNA methyltransferase inhibitors.

### *PARP1 and PARP Inhibition*

PARP1 and the PARP family of proteins are key proteins involved in DNA repair pathways and the maintenance of genomic stability in human cells. Studies into various DNA repair mechanisms, have highlighted PARP1 as protein involved in the recognition of DNA break sites as well as a key protein in the recruitment of DNA repair proteins. General PARP1 activity at DNA break sites has been attributed to an automodification domain within the protein that undergoes self-poly ADP-ribosylation, or the creation of poly ADP-ribose (PAR) chains, known as auto-PARylation (Langelier, 2012). This process is key to the onset of base excision repair (BER), alternative nonhomologous end-joining (Alt-NHEJ), and single-strand break repair (SSBR) which are all driven by the recruitment of PARP1 to sites of single-strand breaks (SSB), double-strand breaks (DSB), and abasic sites (AP) within the DNA (Wang, 2006, Lupo, 2014). The creation of these PAR chains bound to PARP1 creates a scaffold that acts as a recruitment signal for various repair proteins resulting in the formation of the working repair complex, specific to the type of break. Once these proteins are recruited and the repair complex formed, PARP1 releases the PAR chain which signals PARP1 to release from the DNA and initiates the DNA repair process (Figure 1) (Croset, 2013, Javle, 2011).

Inhibition of PARP1 is based upon the idea that, with the loss of PARP1 activity, the cells will lose PARP-regulated DNA repair mechanisms resulting in a buildup of DNA break sites (Kedar, 2012, Muvarak, 2016). The buildup of unresolved DNA breaks, specifically DSBs, can act as a signal for numerous programmed cell death pathways, that in the case of cancer, would result in the death of targeted cells. Inhibition of the PARP1 protein can occur in one of two ways depending on the type of inhibitor. One

method uses a molecule to block the recognition/DNA binding domain of PARP1, which results in no response of PARP1 to break sites. In this case, break sites remain open until either fixed by other repair pathways, like homologous recombination, or cellular dedication to apoptosis. The second method of PARP1 inhibition acts through the blocking of the auto-modification domain. These molecules bind to the auto-modification domain in a way comparable to normal PAR, but are designed to block the inclusion of additional PAR groups. This consequently blocks the creation of the PAR recruitment scaffolding. With the process of PARylation blocked and the PAR chain absent, the repair complexes are not recruited and PARP1 remains bound or trapped on the DNA; a recently identified process known as PARP trapping (Muvarak, 2016, Murai, 2012).

PARP trapping itself is a major goal for many PARP inhibitors as the permanent binding of PARP to the DNA break site leads to the formation of lesions within the DNA (Murai, 2012). Cells undergoing proliferation need to replicate the genetic material before the cell can fully divide. During DNA replication, SSBs and AP sites within the DNA will halt the progression of the replication machinery forcing the replication fork to stall and eventually collapse. The collapse of the replication fork creates a DSB at the site of the stall (Sedletska, 2013). DSBs are much more hazardous towards genomic stability, and buildup of these breaks will eventually result in cell death if they are not repaired fast enough. PARP trapping agents are designed to aid the process of DSB formation. With PARP bound to the DNA, the site of damage already present is blocked by the bound protein which hampers other DNA repair proteins from accessing the site. This results in a semi-permanent DNA lesion that will eventually stall the replication fork

as it passes over the site, resulting in the formation of a DSB as the fork collapses (Figure 1) (Sedletska, 2013, Gaymes, 2009).

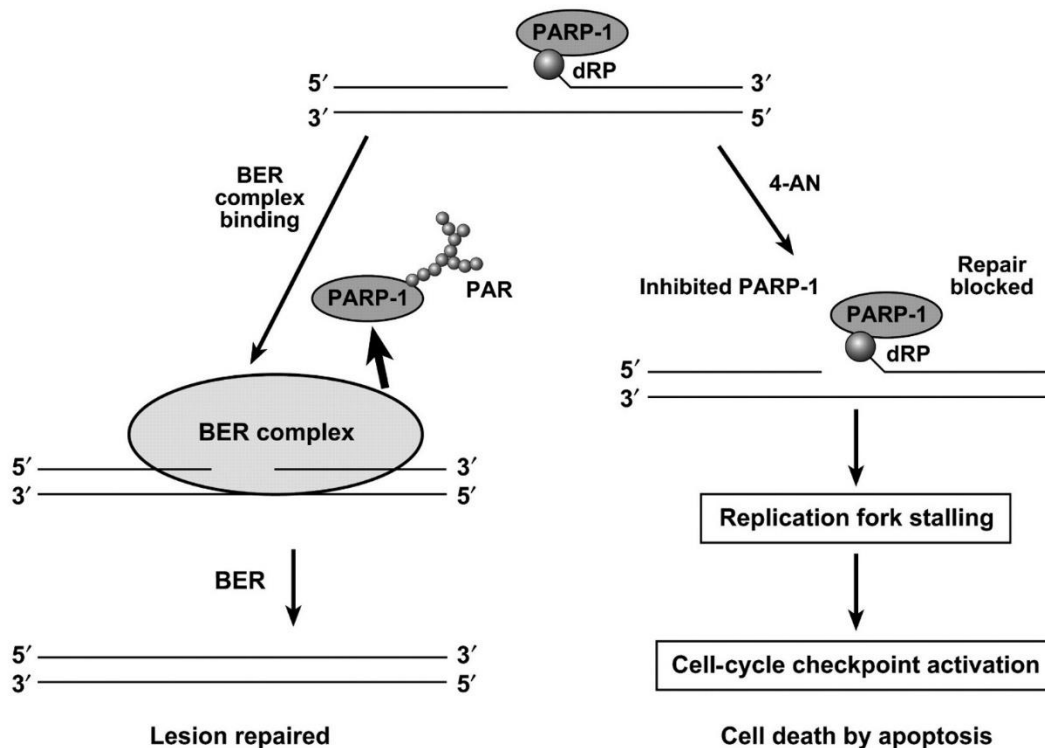


**Figure 1: PARP Inhibition During BER and SSB Repair:** The presence of abasic sites or SSBs recruits and activates PARP1 to bind to the exposed 5'-deoxyribose phosphate group (dRP). Once bound, PARP begins the creation of the repair complex scaffolding via auto-PARylation. The completed PAR chain recruits the BER, or other DNA repair complexes which are then activated upon the release of PARP1 and the PAR chain. During PARP inhibition, in this case by compound 4-AN, the PAR chain cannot be built, inhibiting the recruitment of the repair complex and trapping PARP to the break site. During DNA replication, the replication fork stalls at the break site, eventually collapsing creating a DSB that can activate certain cell cycle checkpoints leading to cell death. **Adapted from Kedar, 2012**

Use of PARP inhibitors as a targeted therapeutic strategy has been growing steadily since the approval of the first clinically effective compound, Olaparib, in 2014. The initial, approved use of Olaparib were for the treatment in ovarian cancer patients with germline mutations in breast cancer type 1 susceptibility protein, better known as

BRCA1 (Kim, 2015). The BRCA family, mainly BRCA1 and BRCA2, are major factors in the repair of chromosomal damage, DNA DSB repair, and the overall maintenance of genomic stability through their roles in the induction of homologous recombination (HR). BRCA-mutant cells lack the ability to repair DSB via HR, and instead must rely on more error-prone methods of repair in order to avert the onset of apoptosis (Helleday, 2011). The use of Olaparib in these patients was effective due in part to the synthetically lethal combination of SSB formation coupled with a lack of effective DSB repair. Synthetic lethality, by definition, is a type of genetic interaction where the simultaneous perturbation of at least two genetic events will result in decreased cellular fitness. However, only when both genetic events are altered is the complete effect on cell survival seen (Nijman, 2011, Leung, 2016). The disruption of these genetic events are not confined to just the gene, but also the gene products and the activities/roles that those products hold in the cell. The implementation of synthetic lethality in the creation of therapeutics usually works through a combination of two independently acting treatments that act upon different cellular pathways that both play a role in the control of certain cellular aspects (survival, proliferation, repair, etc.). With one pathway disrupted, the cell must rely on the second pathway to continue normal function, which creates a cell that is sensitive to agents that can block this second pathway. This increased sensitivity will result in a larger cytotoxic effect, that was not originally possible in the normal, untreated cell. In the case of using Olaparib in BRCA-mutant cells, the introduction of Olaparib would result in SSB formation from PARP trapping within the DNA. These breaks are converted to cytotoxic DSB during replication. The increase in DSB incidence in HR-deficient, BRCA-mutant cells, creates a cytotoxic crisis state in which DSB repair

pathways are overwhelmed, forcing treated cells to become apoptotic (Helleday, 2011). Current research has focused more on the identification of other therapeutic combinations with PARP inhibitors, that can create similar antioncogenic outcomes through synthetic lethality, without the reliance on genetic predispositions in the patient/tumor. These studies have highlighted the ability for PARP inhibitors to sensitize tumorigenic cells to radiation therapies. This sensitization was primarily characterized by increasing levels of tumor cell death in response to low, non-cytotoxic doses of Olaparib. Studies identified that increased prevalence of DNA damage sites correlated with these cytotoxic outcomes. This was attributed to the synthetically lethal combination of targeting DNA repair mechanisms (through PARP1 inhibition) after the formation of SSBs through IR exposure (Verhagen, 2015). The use of PARP inhibitors as radiosensitizers has since been outlined as a possible therapeutic strategy for solid-tumor patients regardless of their genetic background.

As PARP inhibitors continue to play more considerable roles in the creation of more effective cancer therapeutics, likewise has the demand for stronger, more potent compounds has continued grow. Upon the discovery and definition of PARP trapping and its antitumorigenic effects (Murai, 2012), more and more work has gone into developing inhibitors that can bind PARP with more efficiency and specificity. From this work came the identification and development of a compound known as Talazoparib (Tal), previously referred to as BMN 673. Early comparisons in PARP activation and trapping assays, using DT40 and DU145 cells, found that Tal had significantly higher PARP trapping and inhibitory capabilities, compared to previously established PARP inhibitors, Olaparib and Rucaparib (Murai, 2014). The increased potency as a PARP

inhibitor shown by Tal, was closely linked to increased cytotoxicity in cells co-treated with the alkylating agent, methyl methanesulfonate (MMS). Additional studies have looked into the PARP trapping and cytotoxic capabilities of Tal in other cell lines, as well as into the specific mechanisms of inhibition through which Tal acts (Wang, 2016, Shen, 2015). Continued testing has consistently shown Tal to be one of the most potent PARP trapping agents available, which has helped to move Tal into clinical trials, currently undergoing Phase 3 trials.

#### *DNMT1 and DNMT Inhibition*

DNA methyltransferase (DNMT) is another protein linked extensively with epigenetic alterations found in numerous cancer types. Normal DNMT function is characterized as the transfer of methyl-groups, known as methylation, to the 5'-carbon of the pyrimidine ring of cytosine bases within the DNA. The process of DNA methylation is used, relatively universally, as a method of gene regulation without altering DNA sequences. In humans, DNA methylation usually acts as a form of gene silencing, as the binding of methyl groups within a promoter sequence will halt the transcription of genes linked to that promoter (Robertson, 1999). As a matter of fact, many human housekeeping genes that require strict regulation are preceded by promoter regions rich in cytosine and guanine nucleotides. The regions, known as CpG islands, are used exclusively as targets for DNA methylation (Jabbari, 2004).

DNMT1 is the most abundant form of human DNA-methyltransferase, and is the primary protein responsible for the regulation and maintenance of methylation-dependent

epigenetic patterns (Robertson, 1999). Methylation patterns, controlled by DNMT1, play a significant role in the coordinated regulation of several tumor suppressor genes, including *ATM* and *APC*, that drive the cell away from proliferation and towards apoptosis when certain requirements are not met or issues are present (Rigi-Ladiz, 2011, Do, 2014). However, this ability to silence tumor suppressor genes means DNMT1 is frequently associated with certain human cancers. Lung cancer is one of these cancers commonly linked with DNMT1 overactivation. Previous studies have highlighted a trend of hypermethylation within tumorigenic cells, suggesting that altered methylation patterns play some role in the tumorigenicity of a cancer cell (Baylin, 2000).

The hypermethylation patterns seen in various cancers has prompted the development of DNMT inhibitors that are designed to take advantage of this highly active state. One such inhibitor is 5-azacitidine (AZA) which, as with many other DNMTis, closely resembles natural cytidine that can be integrated into the DNA of treated cells during S phase replication (Christman, 2002). Once integrated, these compounds are identified and covalently bound by DNMT for methylation. However, these compounds have a slight variance from natural cytidine in the form of a nitrogen atom at the 5'-position that blocks the addition of the methyl group by DNMT. The binding of DNMT normally signals the cofactor, S-adenosyl-L methionine (SAM), to transfer the methyl group to the 5'-position. With that process blocked, SAM is unable transfer the methyl group and DNMT remains irreversibly bound to the DNA. This method of epigenetic therapy follows a similar focus to the previously mentioned PARP inhibitors. By inhibiting the release mechanism of DNMT there is an increase in the number of protein-bound DNA lesions that are targeted for repair by DNA repair

processes (Issa, 2004). As with the PARP inhibitors, the reliance of DNMT inhibitors on the formation of DNA break sites, make these compounds feasible candidates for combination therapies with other DNA damaging therapeutics. Radiosensitization testing in NSCLC and glioblastoma cell lines found that pretreatment with a DNMTi followed by IR exposure decreased cell survival in clonogenic assays and prolonged expression of DSB marker  $\gamma$ H2AX. This compared to radiation therapies alone. These results were consistent through individual treatment with 3 different DNMT inhibitors, including AZA. (Kim, 2012).

#### *Combination Treatment in NSCLC and Co-treatment with IR*

Based on the ideals of synthetic lethality, it has been proposed that increasing the numbers of DNA lesions, via DNMTi treatment, should in turn upregulate the recruitment of PARP1 to the DNA. When in the presence of a PARP-trapping agent, the recruitment of PARP1 should result in the formation of even more DNA lesions and SSBs, forcing any passing replication forks to stall and eventually collapse (Muvarak, 2016). This process, illustrated in Figure 2, should move the cell into a crisis state due to the dramatic increase in DSB formation that will favor the onset of apoptosis over DNA repair and cell survival.

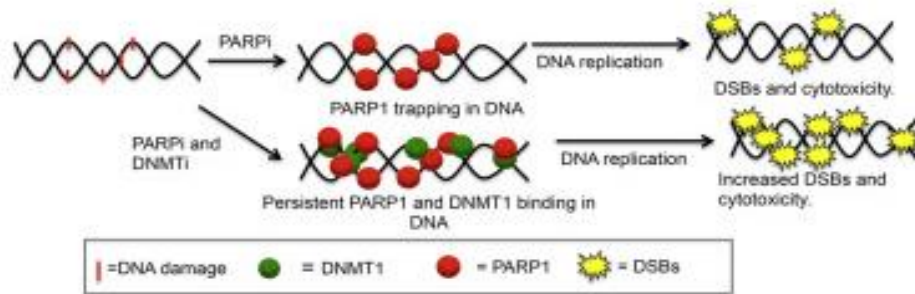


**Figure 2: Co-Treatment with DNMT and PARP Inhibitors:** The presence of PARP inhibitors alone, will trap PARP molecules wherever they are recruited into the DNA. However, this recruitment will only occur when breaks or lesions are present. In a normal state, there will be few of these sites, limiting the effectiveness of the inhibitor. Co-treatment with a DNMT inhibitor will actively create DNA lesions that will act as PARP recruitment sites. Increasing PARP recruitment and eventual inhibition alongside DNMT inhibition, will produce a greater number DNA breaks that should have a more drastic effect on cell survival. **Adapted from Muvarak, 2016.**

Combination therapies with PARP and DNMT inhibitors have been proposed and proven to effectively induce synthetic lethality in numerous cancer types due to their synergistic activity. Previous work in our laboratory has shown that low, non-cytotoxic doses of the PARP inhibitor, Tal, used in combination with the DNMT inhibitor, decitabine, resulted in significantly increased cell death in both acute myeloid leukemia (AML) and breast cancer models (Muvarak, 2016). Results from these studies highlighted a mechanism of action through which PARP1 became trapped at sites of DNA damage which correlated heavily with cell cytotoxicity. Previous studies have also shown that this effect is bolstered when Tal-treated cells are co-treated with low doses of radiation, compared to radiation therapy alone (Albert, 2007). Co-treatment with Tal and IR has also shown to result in increased formation of  $\gamma$ H2AX foci (Wang, 2011). These results further support the argument that PARP inhibitors are highly effective in cells that

are prone to DNA damage, and can be combined with other DNA damaging therapeutics to illicit larger cytotoxic responses.

The combination of Tal with DNMT inhibitors is designed to act as this DNA damaging therapeutic, and has been shown to boost the overall efficacy compared to single agent treatment. The resulting increase in treatment efficacy has allowed for the use of smaller effective dose requirements (Muvarak, 2016). Lowering the dosing requirements for NSCLC treatment should help to limit the off-target side effects that are characteristic of non-targeted therapies, theoretically creating a safer therapeutic strategy. The success of co-treatment with PARP and DNMT inhibitors seen in AML and breast cancers, suggests that this combination could be used effectively in a wide number of different cancer types. This is mainly due to the non-specificity of the combination towards certain tissue types, as BER and Alt-NHEJ are used throughout the human body to repair DNA damage sites. Both Tal and AZA have been independently identified as clinically successful radiosensitizing agents, therefore the combination treatment with radiation therapy should enhance the overall efficacy of both inhibitors, when used in combination. We propose that PARP1 and DNMT1 inhibitors, Talazoparib and 5-azacitidine, used concurrently with low doses of ionizing radiation can be used as an effective therapeutic strategy for NSCLC, due to increased inhibitor efficacy and lower dosing requirements for improved patient survival.

## **Chapter 2: Radiation Enhances Therapeutic Effect of PARPi and DNMTi Combination in NSCLC.**

In this chapter, we performed studies to determine the effectiveness of Talazoparib and 5-azacitidine combination treatment in NSCLC. To do this we used clonogenic colony survival assays in order to measure cell survival. We then introduced a third treatment component in the form of low-dose IR exposure and compared cell survival and clonogenicity against inhibitor treatments without IR. To analyze the mechanisms by which Tal and AZA combination treatment enhance cytotoxic outcomes, we carried out a series of cell viability assays in order to model the synergistic capabilities of co-treatment of the two inhibitors. Further experimentation was done to illustrate the molecular processes and effects that result from treatment with each of our two combinations. We first used immunofluorescent staining of DSB marker,  $\gamma$ H2AX, to study DNA repair processes through the creation and retention of DSBs in inhibitor and inhibitor + IR treated cells.

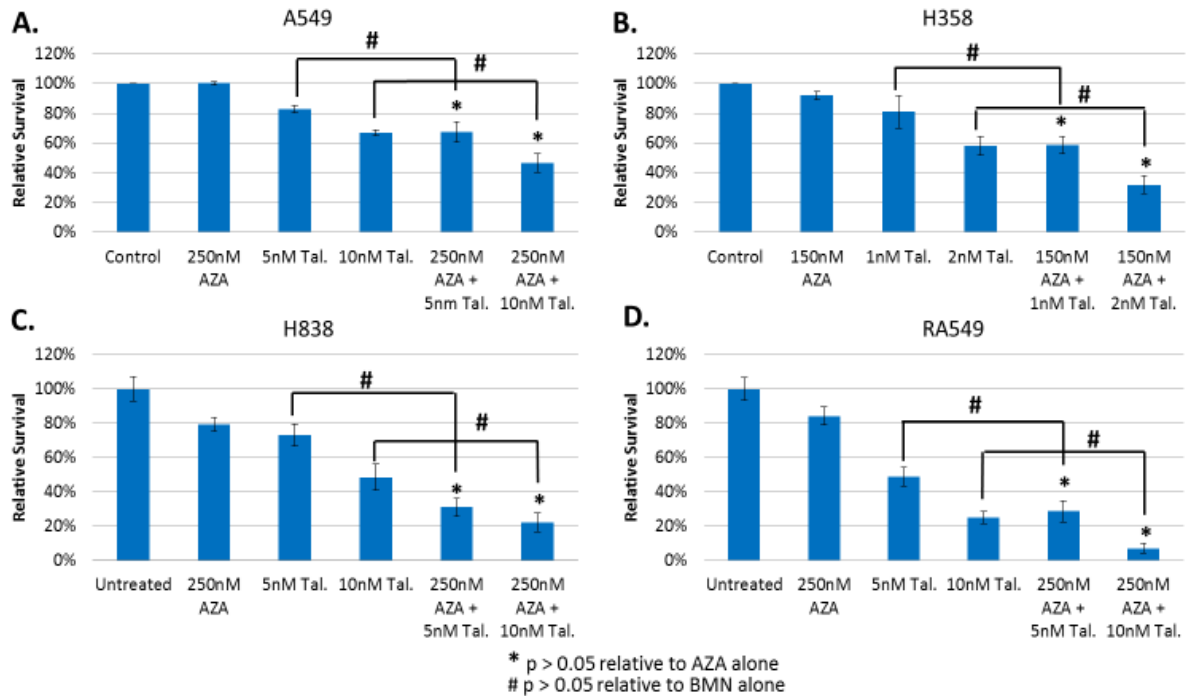


**Figure 3: Combination Treatment with Tal and AZA Reduces Survival and Clonogenicity in NSCLC Cell Lines:** Bars represent average colony count relative to average number of colonies formed in control/nontreated wells. All measurements compared using student’s two-tailed, unpaired t-tests using group-specific standard deviations, represented as +/- error bars.

*Inhibitor Combination Effect on Cell Clonogenicity*

To measure the efficacy of our inhibitor combination, we began analyzing the effects each inhibitor has on the colony formation/clonogenicity of 4 basal epithelial NSCLC cell lines (Figure 3). AZA treatments across all 4 cells lines resulted in negligible effects on cell survival, suggesting limited baseline sensitivity to this DNMT inhibitor. However, cell lines showed higher sensitivities to Tal treatments, especially at higher dose of 10 and 2nM respectively. Initial experiments with cell line H358 using 250nM AZA with 5 and 10nM Tal, highlighted a notable difference in baseline sensitivity to both inhibitors. To compensate for this, later experiments used lower doses

of both AZA and Tal to maintain accuracy. Nonetheless, at these lower doses, H358 followed a similar trend with AZA and Tal sensitivity (Figure 3B).

Survival data from AZA and Tal combination-treated wells concluded that use of PARP1 and DNMT1 inhibitors in combination increased overall treatment efficacy when compared to single agent treatments (Figure 3A-D). This increase in efficacy is characterized by significant decreases in colony formation seen across all 4 cell lines. The addition of previously ineffective doses of AZA to semi-effective doses of Tal resulted in a significant decrease in survival when compared to either drug alone ( $p < 0.05$ ). Similar trends in all 4 cell lines show that the combination of low dose Tal (1 or 5nM) with AZA results in an effect that is comparable to Tal treatments at a 2x higher dose (2 or 10nM respectively). Results from these clonogenic assays suggest that the combination treatment of Tal and AZA together produces a greater effect against NSCLC clonogenicity and tumorigenicity.

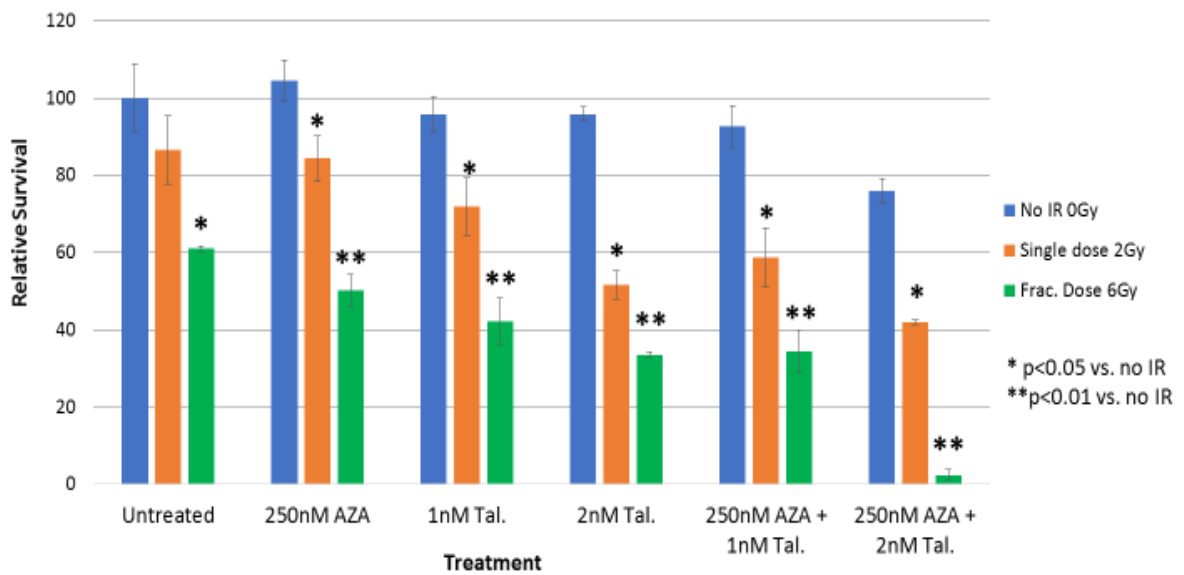


**Figure 4: Introduction of IR Further Reduces Clonogenicity in NSCLC Cells:** Colony survival assay completed with A549 cells with addition of a 2Gy single dose IR (orange), or fractionated 6Gy dose IR (green). Relative survival measured as average colony count relative to average number of colonies formed in control/nontreated wells. Measurements for each treatment group reported as average percent survival  $\pm$  SD. Statistical significance measured via student’s two-tailed t-test.

*Co-treatment with IR Decreases Clonogenicity of PARPi and DNMTi Combination*

Given that IR creates more single stranded breaks, we would expect that this increased DNA damage would recruit more PARP that would then be targeted by PARP and/or DNMT inhibitors (Muvarak, 2016). Therefore, as in Figure 3, colony survival assays were used to assess if the introduction of IR would increase the effectiveness of AZA or Tal individually or in combination. The introduction of radiation into combination-treated cells resulted in drastic increases in overall efficacy while also following a similar dose-response trend seen in non-irradiated, combination-treated cells (Figure 4). Across all treatment combinations, wells given an additional single dose IR

(orange) produced notably decreased clonogenicity, compared to non-irradiated, inhibitor-treated wells, shown in blue ( $p < 0.05$ ).

Further testing using larger, fractionated doses of IR produced even greater responses in cell clonogenicity. All AZA/Tal treatment combinations co-treated with 6Gy (green) led to decreased cell survival, compared to both non-irradiated ( $p < 0.01$ ) and single dose 2Gy irradiated cells ( $p < 0.05$ ). Most notably, the largest dose combination (250nM AZA with 2nM Tal) with fractionated IR, produced one of the largest differences in clonogenicity. Combination and IR treatment resulted in 2% survival, an average difference of over 70% compared to the non-irradiated combination.

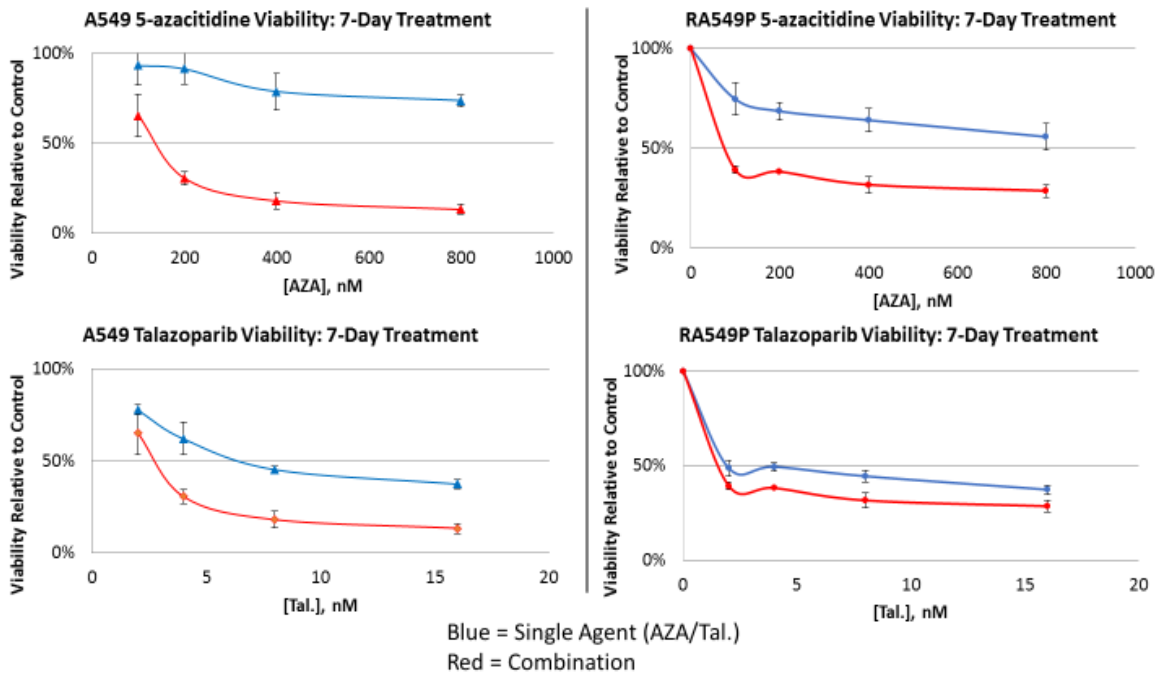


**Figure 5: MTS Analysis of PARPi and DNMTi Combination Treatment:** Blue lines represent the relative viability of cells exposed to a single agent (either AZA or Tal) at increasing doses. Red lines represent the relative viability of cells exposed to the combination of Tal and AZA at the same increasing doses. Viability measurements obtained by measuring the absorbance at 490nm of test group relative to that of the control group (no drug). Reported as relative viability  $\pm$  SD.

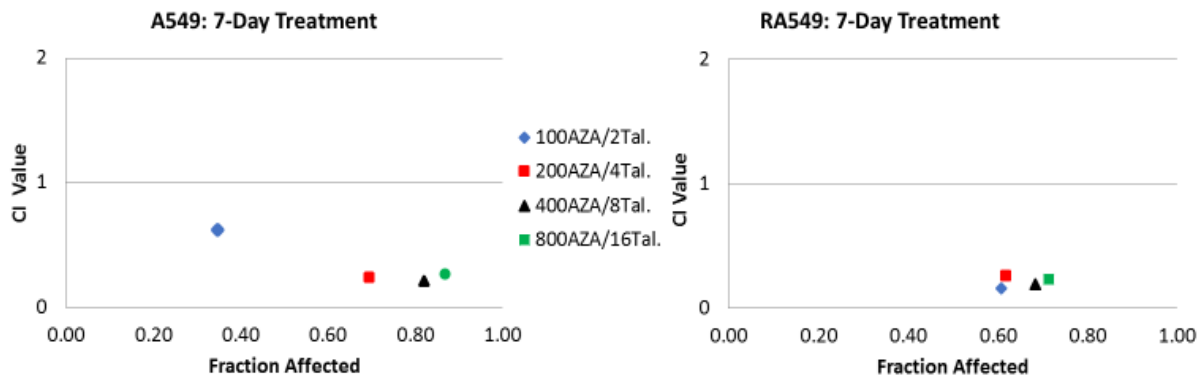


**Figure 6: Co-Treatment with PARPi and DNMTi Show Synergistic Relationship:** MTS fraction affected measurements used to calculate the CI value at each individual dose combination. Corresponding CI values for both cell lines ( $CI < 1$ ) show combination treatment with 5-azacitidine and Talazoparib is synergistic within the dose range of 100nM/2nM to 800nM/16nM (AZA/Tal).

#### *Synergistic Relationship Between PARPi and DNMTi Combination*

Many novel therapeutic combinations are specifically designed to act on a similar target molecule or pathway in order to boost the combined effectiveness beyond either component alone. This is known as synergy. A series of cell viability/MTS assays were completed with increasing concentrations of AZA and Tal (Figure 5). Responses to increasing doses of the combination and AZA/Tal alone were used to model the synergistic relationship between both inhibitors (Figure 6) (Chou, 2006).

MTS assays run with A549 and RA549 cells, showed a decrease in cell viability with increasing doses of AZA and Tal both alone and in combination (Figure 5). The synergistic score of the Tal-AZA combination was determined from MTS measurements using the Chou-Talalay model of additivity (Chou, 2006). This model uses the fraction affected (0.40 when measuring 60% cell viability) to measure the ratio of dose to effect

(Dose of inhibitor : Fraction affected). The ratios of both component inhibitors are then combined to create the combination index or CI value. Combinations with CI values greater than 1 are considered antagonistic, while CI values less than 1 are considered synergistic. CI values for all doses of AZA and Tal in A549 cells sat below a value of 1; this suggests a synergistic relationship across all dose combinations (Figure 6). The same was seen across all dose combinations for RA549. The leftwards shift of all data points for RA549, compared to A549, suggests a steeper dose response and higher sensitivity to AZA and Tal showing larger fractions affected at smaller doses.

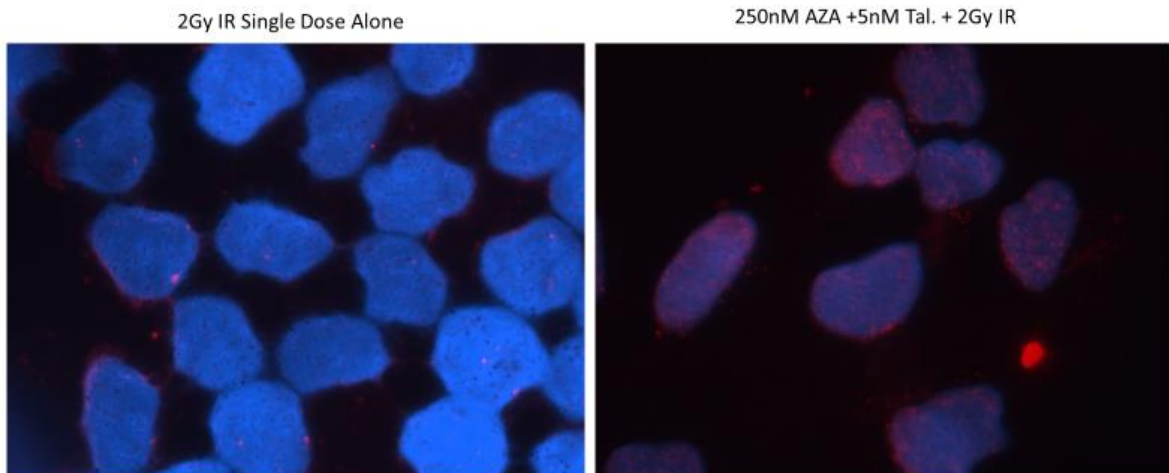


**Figure 7: IF-Stained  $\gamma$ H2AX Foci in RA549 NSCLC Cells:** Fluorescent images taken of RA549 cells fixed 1 hour after 2Gy IR. Image on left was incubated 7 days in media only. Image on right was incubated for 7 days in 250nM AZA and 5nM Tal prior to 2Gy IR. Nuclear DAPI staining highlights cell nuclei seen as blue circles.  $\gamma$ H2AX foci are seen as small red dots within each nucleus.

## *Molecular Analysis of Therapeutic Effects*

The combination of PARP and DNMT inhibitors leads to an increase in cytotoxic DNA double-strand breaks, as assessed by DSB-marker,  $\gamma$ H2AX (Muvarak, 2016).  $\gamma$ H2AX foci form at sites of DSBs which can be quantified following exposure to DNA damaging agents as a measure of DNA damage.  $\gamma$ H2AX foci resolution and retention can also be used to indirectly assess DNA repair or lack thereof. Immunofluorescent (IF) staining was used to link  $\gamma$ H2AX foci with fluorescent tags in order to create a quantitative measure of DNA damage and response to the AZA and Tal combination in NSCLC cells. A time course of 1, 4, and 24 hours was completed in order to measure both the foci formation (at 1hr post-IR) and retention over the course of 24 hours after radiation. Each sample coverslip was divided in 4 quadrants that were each considered a distinct population of that specific treatment group. Multiple images of each quadrant were taken with fluorescent microscopy under DAPI and TRITC-exciting lights (UV and yellow-green respectively) then the number of foci (TRITC) per nucleus (DAPI) were quantified via counting software. The resulting IF images of irradiated, untreated and combination treated cells can be seen above in Figure 7.

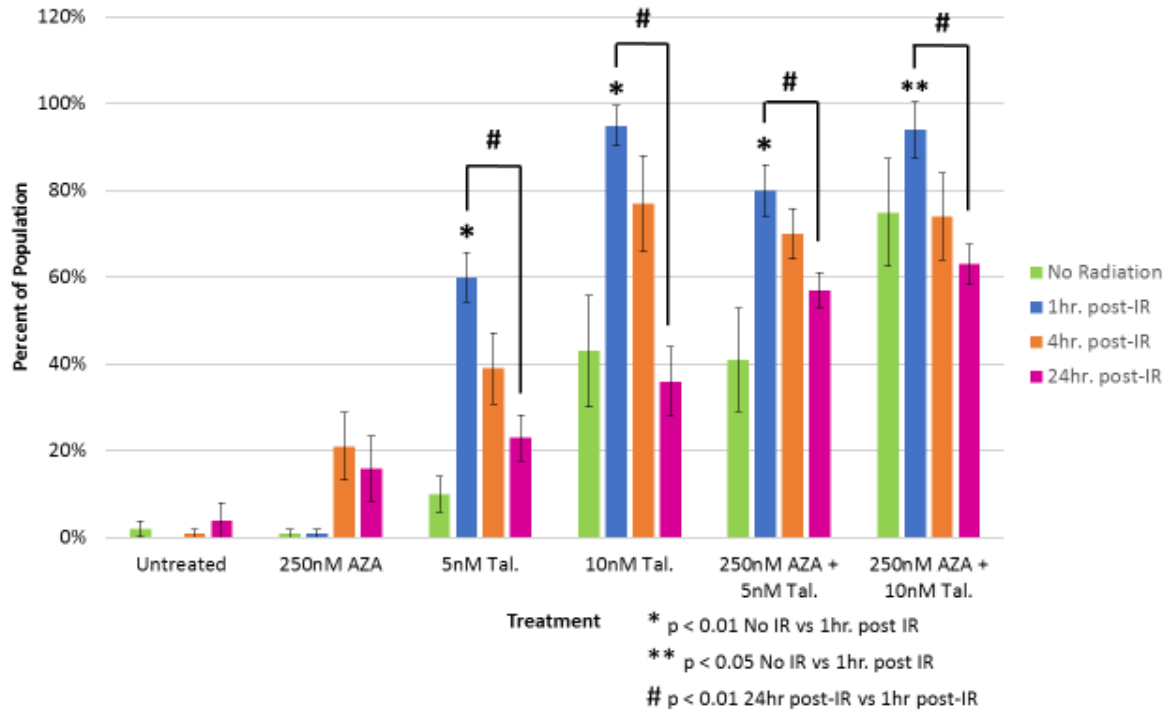


**Figure 8: PARPi and DNMTi Treatment in Combination with Single Dose IR Increases  $\gamma$ H2AX Foci Formation and Extends Retention Time:** Bars represent percent of cell population that exhibit  $\geq 20$  foci within a single nucleus. Green bars represent non-irradiated, treated cells. Blue, Orange, and Purple bars represent cells that received an additional single 2Gy dose IR, then were collected 1hr., 4hr., and 24hr. post-IR respectively. All measurements reported as average percent of quadrant population  $\pm$  SD. Significance measured via student’s two-tailed t-test.

Figure 8 above outlines  $\gamma$ H2AX foci formation and retention in response to IR with and without the AZA-Tal combination. Results are represented as percent of sample population exhibiting  $\geq 20$  foci per cell/nuclei. Combination treated groups showed significantly higher foci counts prior to radiation compared to corresponding AZA and Tal treatments alone ( $p < 0.01$ ). Introduction of a single 2Gy dose resulted in a significant increase in foci formation after 1 hour post-IR in all Tal and combination groups ( $p < 0.05$ ). The increased foci formation suggests that introduction of IR into inhibitor-treated cells increases DSB formation. Comparisons of foci retention times

between Tal-treated and combination-treated cells found a significant increase in foci retention time in cells receiving both AZA and Tal ( $p < 0.05$ ). The increased retention time suggests that DNA repair is impaired to some extent in combination treated cells.

### **Chapter 3: Concurrent Radiation Therapy Increases Efficacy of Inhibitor Combination In Vivo.**

In the previous chapter, we looked to measure the efficacy of PARP and DNMT inhibitor combinations in NSCLC *in vitro* and looked to boost that efficacy through the addition of low doses of IR. Results from those experiments suggested that using this combination as a treatment protocol could be advantageous in treatment of NSCLC. However, in order to examine if the integration of this treatment protocol will result in equally positive patient outcomes, tested the two inhibitors and IR combination in an *in vivo* mouse model. In this chapter, we developed two independent treatment protocols, each using the AZA and Tal combination with either 2 or 6Gy IR, and tested for treatment efficacy in nude mice with subcutaneous human NSCLC xenografts. These experiments were designed to analyze the effectiveness of the combination with IR compared to each component individually. Treatment efficacy was measured by tumor volume versus time, and time to endpoint (TTE) which is the time to reach a certain tumor size. Changes in body weight we also monitored to ensure that the treatments were tolerable.

Our first study was focused on testing the effect of the combination(AZA/Tal) with a single, 2Gy dose of IR. Forty female nu/nu (nude) mice were given subcutaneous injections of 1 million RA549 cells on their right flank. After tumors reached an approximate volume of 100mm<sup>3</sup>, mice were divided into one of four treatment groups so that mean tumor volume was similar. Treatment groups are outlined below (Table 1).

<b>Group</b>	<b>Treatment</b>	<b>Dose</b>	<b>Route of Administration</b>	<b>Schedule</b>
1	Control	-		
2	IR Alone	2Gy IR	External Beam	One Dose
3	AZA/Tal	0.5 mg/kg AZA 0.3 mg/kg Tal	SC (subcutaneous) PO (oral)	5 days/week 5 days/week
4	AZA/Tal/IR	0.5 mg/kg AZA 0.3 mg/kg Tal 2Gy IR	SC PO External Beam	5 days/week 5 days/week One Dose

Groups 3 and 4 were pre-treated for 5 days with AZA/Tal prior to radiation. On the 6<sup>th</sup> day, tumors were irradiated(2Gy) with a single dose of IR using the small animal radiation research platform (SARRP). Tumors in groups 2 and 4 were irradiated once the mean tumor volume reached approximately 400mm<sup>3</sup>. Tumor volume and weight were measured twice a week. Mice were treated until the tumors reached 1500mm<sup>3</sup> as measured by electronic calipers. At this point, the mice were euthanized and removed from the study; the tumor tissue was excised and fixed and frozen for future pharmacodynamic studies.

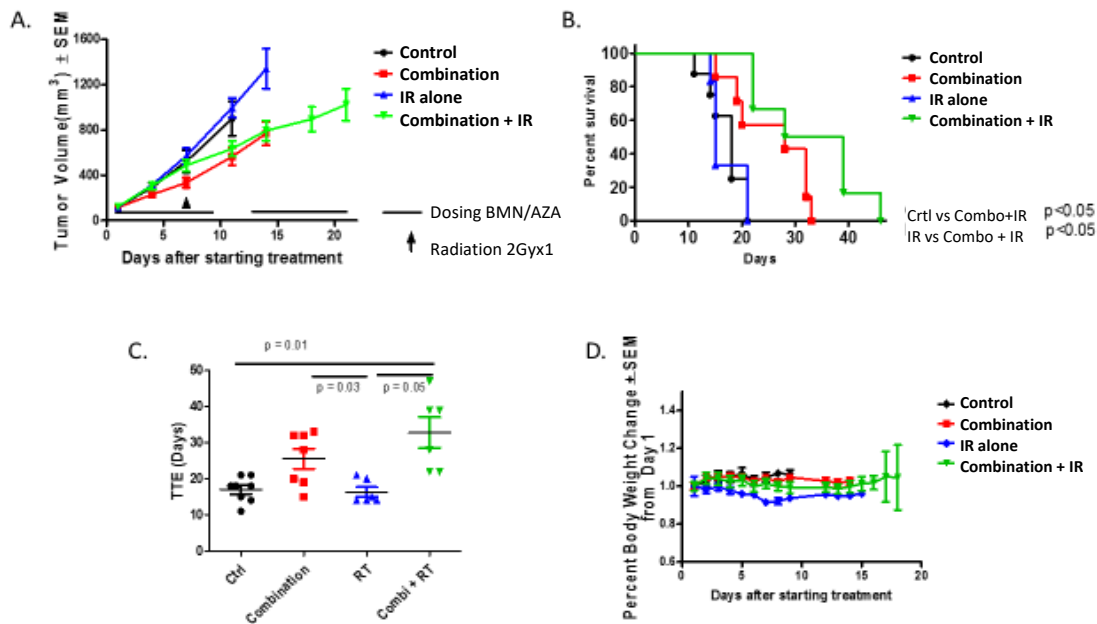


**Figure 9: Addition of Single Dose IR Failed to Alter Efficacy of PARPi and DNMTi Combination Treatment:** **A.** Tumor volume (mm<sup>3</sup> ± sem) vs time (days). **B.** TTE as shown in a Kaplan-Meier survival graph (percent survival vs. time) **C.** Individual time-to-endpoint (TTE) measurements for each treatment group. Symbols represent individual tumors with the group mean shown as a solid line with SEM error bars. **D.** Change in body weight vs time. Each point within the line represents mean ± sem.

Concurrent treatment with AZA and Tal with IR lead to significant increases in survival time over nontreated mice ( $p < 0.05$ ) (Figures 9B, 9C). Significant increases in survival time were also observed in AZA/Tal combination with IR when compared against IR alone and AZA/Tal combination alone ( $p < 0.05$ ) (Figure 9C). However, the *in vivo* use of AZA and Tal in combination with single dose IR did not significantly effect tumor growth in treated mice (Figure 9A-C). Single dose radiation alone had a minimal effect on tumor progression as can be seen with tumor volume (Figure 9A), animal survival (Figure 9B), and the TTE individual data (Figure 9C). The combination of AZA and Tal had a modest, but not significant effect on tumor growth and addition of single dose IR increased survival and delayed tumor growth (Figure 9B-C) compared to

control and IR alone. It was noted, however, that both combination and combination with IR treatments were tolerated well (Figure 9D).

Despite the increased rates of survival (Figure 9B) and minimal toxicity (Figure 9D), the lack of significant tumor reduction suggests the use of AZA and Tal with a single dose of 2Gy IR is not an effective treatment plan for NSCLC in this model. As with our previous *in vitro* experiments, we then attempted to integrate larger doses of IR in order to induce a greater effect on tumor progression/survival. In order to increase IR doses safely, we continued to follow clinical practices with fractionated IR to reduce dose size given at a single time to limit off target toxicities. To test for changes in tumor survival in response to larger dose of IR, a second experiment was designed similar to the first using identical doses of AZA and Tal, but dosing IR-treated mice with three fractionated IR (FIR) doses at 2Gy, instead of one. A second group of 40 mice were injected with 1 million RA549 cells on the right flank. When tumors reached approximately 70mm<sup>3</sup>, mice were divided into the same 4 treatment groups, with groups 3 and 4 pretreated with 6 days of the AZA/Tal combination as described above. On days 7-9, mice in groups 2 and 4 received 2Gy doses IR using the SARRP for a total of 6Gy over three days. Tumor volumes were measured over time and TTE was recorded when tumors reached 1500mm<sup>3</sup> in volume. Once this mark was met, mice were removed from the study and euthanized. Tumor volumes were measured twice a week and weight measurements were taken 5 days per week (every day the mice were dosed with AZA/Tal).

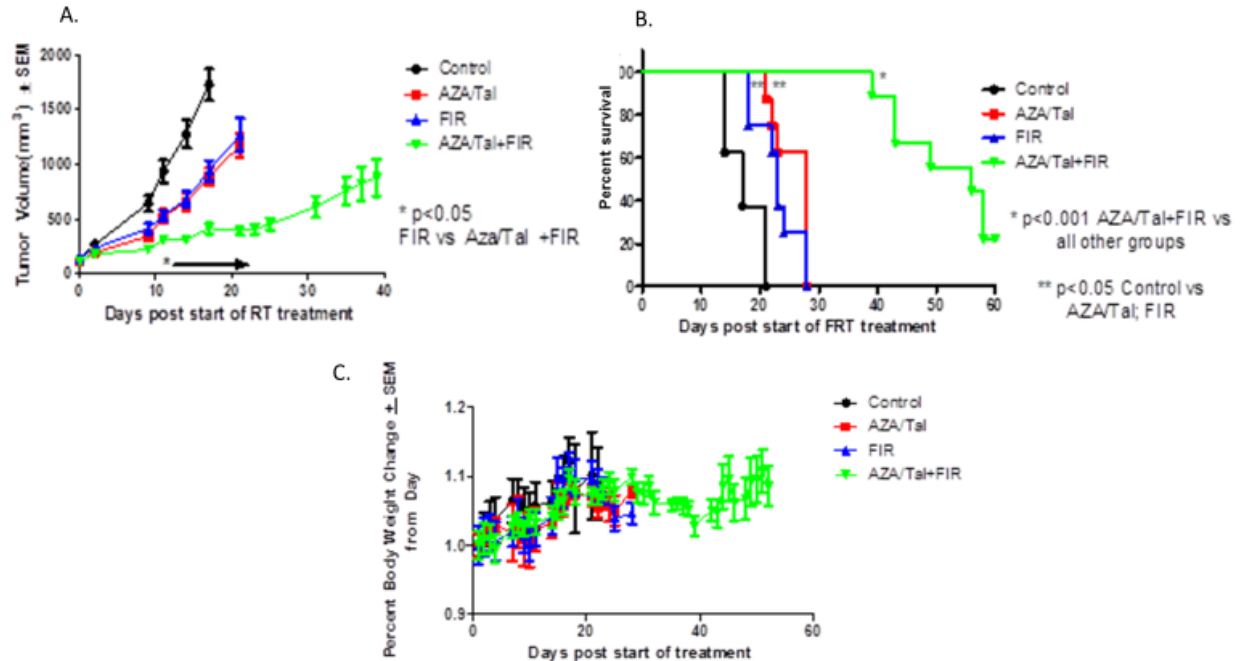


**Figure 10: Fractionated IR in Combination with PARPi and DNMTi Delayed Tumor Growth:** Experimental design matches that seen in Figure 9. Mice receiving IR treatment received one fractionated 6Gy dose split over 3 consecutive days. **A.** Tumor volume (mm<sup>3</sup> ± sem) vs time (days). **B.** TTE as shown in a Kaplan-Meier survival graph (percent survival vs. time) **C.** Change in body weight vs. time. Measurements for data represent mean ± sem.

The addition of fractionated doses of IR for a total of 6Gy had significant impact on measurements of tumor progression (Figure 10A) and TTE (Figure 10B). By increasing the IR dose in combination treated mice, we were able to significantly slow tumor growth rates compared to non-treated mice and each modality alone (p<0.05) (Figure 10A, 10B). While the AZA/Tal combination and IR alone significantly slowed tumor growth compared to no treatment, the combination of AZA and Tal with FIR was the most efficacious treatment, significantly delaying tumor growth compared to each modality alone (p<0.001) (Figure 10B). Co-treatment with our combination and 6Gy FIR managed to slow tumor progression enough to extend measurement times to 40 days, double the time seen in IR only and combination only treatment groups. The combined treatment of AZA and Tal with FIR was also well tolerated (Figure 10C).

## Chapter 4: Discussion

Development of successful NSCLC therapies have proven difficult due to harmful effects at high therapeutic doses, and ineffective outcomes at lower doses (Palma, 2013, Rodrigues, 2004). This has led to the development of the chemoradiation paradigm; using multiple therapeutics with reduced toxicity profiles to better survival rates. Resulting IR combinations with chemotherapeutic compounds like cisplatin and vinblastine found minimal increases in local control rates (average of 4%), yet no significant increases in 5-year survival rates versus radiation therapy alone (Eberhardt, 2006). Successful treatment of NSCLC will require targeted therapies that can limit toxicity while maintaining overall efficacy. The combination of Tal and AZA with low dose IR has met these requirements both *in vitro* and *in vivo*, and has the capability to become a successful therapeutic option for NSCLC.

While the Rassool laboratory showed that the Tal/AZA combination had significant effects on tumor growth and survival in AML and breast cancer *in vitro* and *in vivo*, NSCLC required the addition of low doses of radiation to demonstrate this treatment efficacy. The differences in responses between these cancers may be due to the underlying molecular changes seen in these tumors. Studies into NSCLC progression have concluded that 51% of 72 driver mutations were associated with DNA and histone modification, with a significant portion being involved in DNA repair pathways. This list of susceptible repair proteins included PolE in mismatch repair, FANC and M in homologous recombination, and ERCC5 in base excision repair. All four of these proteins experienced significant alteration frequencies in adenosquamous and squamous cell carcinomas (Jamal-Hanjani, 2017). It has been hypothesized that these altered rates

of expression play a role in the repair of DNA damage that occur during tumor development and may aid in the decreased sensitivity to DNA damaging agents.

The effectiveness of PARP and DNMT inhibitor combinations in multiple cancer types is rooted in the targeted mechanisms through which both inhibitors work. Both inhibitor types have been tested and proven as radiosensitizing compounds (Kim, 2012, Albert, 2007), and this has been attributed to the specific effects of PARP and DNMT inhibition in IR-treated cells. PARP inhibitors inhibit repair of DNA damage that will increase the formation of cytotoxic DSBs. DNMTs inhibit DNA methylation, reprogramming the genome, resulting in cells with altered responses to DNA damage (Tsai, 2012). While these inhibitors have been shown to be radiosensitizers, they have not been successfully translated into effective treatments for NSCLC. The Rassool laboratory published that PARP and DNMT inhibitor combination may work synergistically by a novel mechanism (Muvarak, 2106), by trapping potentially cytotoxic protein-DNA complexes at sites of DNA damage. Therefore, the increased IR exposure combined with the Tal/AZA inhibitor treatment could increase the formation of protein-DNA complexes, leading to increased cell death in NSCLC.

In lung cancer, it is apparent that concurrent use of low dose IR is essential for a complete therapeutic effect with AZA and TAL. Past studies looking to quantify the creation of DNA damage in response to IR exposure, concluded that a single 2Gy dose of IR could result in the formation of 100 cytotoxic DSBs with an additional 1000 non-cytotoxic SSBs (Roots, 1985). The numerous sites of DNA damage will recruit and activate PARP1 (Santivasi, 2014, Langelier, 2013). In the presence of a PARPi, PARP1

becomes trapped at the SSB sites, impairing repair and resulting in the eventual formation of a DSB as the replication fork stalls and collapses (Sedletska, 2013). With the addition of IR, AZA and Tal-treated cells experience a significant increase in DSB formation (Figure 8) with a resulting drop in cell survival (Figure 4). Larger, fractionated doses of IR are expected to create even larger quantities of DNA damage and, when used with AZA and Tal, will produce significant increases in PARP-DNA complexes, that are difficult to repair, leading to decreased cell survival. Our measurement of  $\gamma$ H2AX foci, markers of DSB damage, show that combination drug treatment and IR lead to a sustained foci levels even 24 hours after exposure. This suggests that DSBs remain unrepaired. Further studies elucidating the nature of the repair problem could be achieved by examining DSB repair activity in these cells, following drug treatments and IR, using GFP reporters (Bennardo 2012).

Additional future studies also include apoptosis and PARP trapping assays in order to outline the actual cellular effects that result from treatment with Tal and AZA. Previous studies have outlined these effects in other cancer types (Muvarak, 2016, Helleday, 2011, Wang, 2016), but none of which have been done with this combination in NSCLC cell lines. We are also currently working on genetic expression analyses via microarray on combination and IR treated cells in order to outline the specific responses to DNA damage, resulting from combination and IR treatment. We hope this may help us to explain different baseline sensitivities seen in Figure 3, and possibly identify specific genetic or molecular markers that will determine how certain patients may respond to our proposed strategy.

The initial work done by the Rassool laboratory found that the combination of AZA and Tal alone was effective in AML and breast cancer models (Muvarak, 2016). However, the DNA damaging effects of radiation/IR therapy offers a unique benefit for NSCLC treatment. Radiation therapy in AML patients is rather uncommon, due to the systemic nature of the disease. IR dosing in AML is limited to patients in which the disease has spread to certain organs, like the brain, or created an extramedullary tumor, known as myeloid sarcoma (Almond, 2017). Whole body/systemic radiation exposure is unfeasible, so IR therapy offers little to most AML patients. However, radiation therapies offer more in solid tumor patients and current technological advancements have bettered our ability to target and dose patient tumors with much greater accuracy. One such advancement is the development of stereotactic ablative radiotherapy (SABR). SABR is a highly-focused form of radiation therapy that uses tumor imaging and identification in order to accurately deliver intense doses of radiation to the center of a solid tumor while limiting the exposure to surrounding tissues (Mahmood, 2013, Palma, 2013). The increased accuracy in tumor-targeted dosing has made radiation therapy in combination with AZA and Tal a safer and increasingly effective NSCLC treatment strategy. *In vivo* studies using fractionated, sub-clinical doses of IR in combination with AZA and Tal showed that animals experienced significant decreases in tumor progression (Figure 10A) and increased post-treatment survival (Figure 10B). All IR-receiving mice were irradiated using a small animal radiation research platform (SARRP), an animal-specific type of SABR. This tool allowed us to ensure that all tumors received the complete 2Gy dose when given, and limit unnecessary exposure to surrounding tissues. By limiting the exposure to surrounding tissues, mice exhibited little to no toxicity in

response to either IR or combination (Figure 10C). This limited toxic response, coupled with decreased tumor growth and exceptional post-treatment survival, highlights the immense clinical opportunities that the low dose IR-enhanced, AZA/Tal combination can offer as a NSCLC therapy.

Moving pre-clinical studies from bench to bedside requires multiple steps. Efficacy of the two drugs in combination with IR first needs to be demonstrated in primary patient tumors, such as patient-derived xenografts (PDX). Examining the effects of AZA/Tal and IR in orthotopic models would allow us to elucidate effects on surrounding normal tissue. Given that Tal/AZA in combination with IR have never been used before to treat NSCLC, a dose-finding Phase 1 clinical trial would be necessary. With this trial, we hope to gain a better understanding of possible toxicities and develop a more clinically relevant treatment scheme for human patients.

In conclusion, our data suggests a promising therapeutic strategy of combining Tal and AZA with IR for radiosensitization of NSCLCs. These studies will guide future transition to studies in PDX models and phase 1 dose-finding studies, for future use of Tal/AZA/IR as definitive therapy for NSCLC.

## Chapter 5: Materials and Methods

### *Cell Culturing and Culture Maintenance*

All NSCLC cell lines were grown filtered, 1X RPMI basal media with L-glutamine (Corning) with 10% FBS and 1X penicillin-streptomycin (Corning). Cultures were kept and grown at 37°C and 5% CO<sub>2</sub>. When in culture, cells were subcultured using 0.05% Trypsin, 0.53mM EDTA (Corning). Before seeding any experiment, cells were trypsinized, collected, and resuspended in media. A small volume of cell suspension was added to an equal volume of Trypan Blue solution (Thermo). Cell mixture was placed into hemocytometer and counted to calculate cell density. Stock solution was then diluted to desired seeding density then plated according to experimental protocol.

### *Inhibitor Preparation and Storage*

5-azacytidine/AZA (Sigma) is prepared at 500µm in PBS and stored at -80°C.

Talazoparib, obtained from Medivation, was prepared at 5mM or 50mM in DMSO and stored at -80°C after resuspension.

### *In vitro Irradiation*

All *in vitro* experiments were irradiated using a Pantak photon irradiator. Dose calibrations were carried out daily, before every use, through dosimeter measurements via ionization chamber probe. Probe was exposed to three, 1 minute exposures and average dose(nC/kg)/min was calculated. Using the reported ambient temperature and pressure, average dose was converted to Gray (Gy) and used to determine dose(Gy)/min. These rates were used to set exposure time for irradiated samples. Fractionated 6Gy IR

was given as 3 individual 2Gy doses over 3 consecutive days with 24 hours between each dose. All media, including drug treatments, was removed and replaced within an hour of every radiation treatment.

### *Clonogenic Assays*

Colony survival assays were carried out in 6 well, tissue culture treated plates (Sigma). Cells were plated at a density of 500 cells/well in a final volume of 2mL. Each plate was designated for one of 6 single agent or combination treatments with AZA and Tal. First introduction of the drugs occurred 24 hours after plating by removing old media and replacing with new media containing designated drug treatment. Drug concentrations were maintained over 7 days: AZA was replaced daily, Tal was replaced every third day. Samples receiving an additional single dose IR were irradiated 24 hours after initial drug introduction (72 hours after plating). Samples receiving a fractionated 6Gy IR were dosed on days 4, 5, and 6 to ensure cells are able to settle and grow before dosing. On day 7, plates were collected and stained with a 0.05% crystal violet solution for at least 30 minutes until colonies were fixed and visible. Colonies were counted using the ProtoCol3 program.

### *Cell Viability Assays and Synergy Analysis*

For MTS assays, cells were plated in tissue culture treated 96 well plates (Sigma) in triplicate at a density of 200 cells/well. Each triplicate was set for either control, AZA, Tal, or combination treatment. AZA doses were set at 100, 200, 400, and 800nM. Tal doses were set at 2, 4, 8, and 16nM. The combination groups received both AZA and Tal

at corresponding doses of 100nM AZA+2nM Tal, etc. AZA and Tal treatments were introduced to all treatment wells 24 hours after plating and replaced daily with complete media replacement. Cells were cultured for a total of 7 days with all drug treatments. Assay was terminated using CellTiter96 MTS reagent (Promega) at 20 $\mu$ L/well. Plates were incubated at 37°C for 30 minutes then measured for absorbance at 490nm. Absorbance measurements were made relative to the untreated control wells and used to determine the fraction of affect cells. These values were used to calculate CI values according to the Chou-Talalay method, using the CompuSyn software.

#### *Immunofluorescent Staining*

Cells were plated onto 22mm human fibronectin coated coverslips (BioCoat/Corning). Coverslips were placed into 6 well plates followed by cell seeding at varying densities between 5000 and 7000 cells/well, depending on treatment efficacy. Cells were given 24 hours to settle onto coverslips before introduction of AZA, Tal, or combination into designated wells. AZA and Tal treatments continued for 7 days before coverslip collection on day 7. IR-treated coverslips were irradiated on either day 6 or day 7 depending on desired time point. Coverslips were fixed for 10 minutes with 4% paraformaldehyde; fixation began 1, 4, or 24 hours after irradiation in IR-treated samples. Coverslips were then washed in DPBS and permeabilized for 10 minutes in permeabilization solution (50mM NaCl, 3mM MgCl<sub>2</sub>, 10mM HEPES, 200mM Sucrose, and 0.5% Triton X-100 in PBS 1X). Coverslips were then washed again in DPBS + 1% BSA + 0.1% Triton X-100, then blocked for 1 hour at 37°C in 10% FBS in DPBS. After blocking cells were washed again and left overnight in DPBS + 1% BSA. The following

day coverslips were removed from the 6 well plates and placed into humidity chambers. Coverslips were then incubated with a mouse monoclonal anti- $\gamma$ H2AX antibody (1:100, Millipore) at 37°C for 1 hour. After incubation, coverslips were washed again in DPBS +1% BSA then incubated with a fluorescent anti-mouse secondary antibody (1:200) for 45 minutes at room temperature. Coverslips were then washed one final time in DPBS + 1% BSA + 0.1% Triton X-100 and placed onto glass slides using Prolong (R) Gold Antifade with DAPI Vectashield (Cell Signaling Technologies) and set to dry for 24 hours. Slides were then sealed and analyzed under a fluorescent microscope using the NIS Elements software.

## References

- Albert JM, Cao C, Kim KW, Willey CD, Geng L, Xiao D, *et al.* Inhibition of poly(ADP-ribose) polymerase enhances cell death and improves tumor growth delay in irradiated lung cancer models. *Clin Cancer Res* 2007;13(10):3033-42 doi 10.1158/1078-0432.CCR-06-2872.
- Almond LM, Charalampakis M, Ford SJ, Gourevitch D, Desai A. Myeloid Sarcoma: Presentation, Diagnosis, and Treatment. *Clin Lymphoma Myeloma Leuk* 2017;17(5):263-7 doi 10.1016/j.clml.2017.02.027.
- Baylin SB, Herman JG. DNA hypermethylation in tumorigenesis: epigenetics joins genetics. *Trends Genet* 2000;16(4):168-74.
- Bennardo N, Cheng A, Huang N, Stark JM. Alternative-NHEJ is a mechanistically distinct pathway of mammalian chromosome break repair. *PLoS Genet* 2008;4(6):1000110 doi 10.1371/journal.pgen.1000110.
- Chou TC. Theoretical basis, experimental design, and computerized simulation of synergism and antagonism in drug combination studies. *Pharmacol Rev* 2006;58(3):621-81 doi 10.1124/pr.58.3.10.
- Christman JK. 5-Azacytidine and 5-aza-2'-deoxycytidine as inhibitors of DNA methylation: mechanistic studies and their implications for cancer therapy. *Oncogene* 2002;21(35):5483-95 doi 10.1038/sj.onc.1205699.
- Croset A, Cordelieres FP, Berthault N, Buhler C, Sun JS, Quanz M, *et al.* Inhibition of DNA damage repair by artificial activation of PARP with siDNA. *Nucleic Acids Res* 2013;41(15):7344-55 doi 10.1093/nar/gkt522.
- D'Amico TA, Massey M, Herndon JE, Moore MB, Harpole DH. A biologic risk model for stage I lung cancer: immunohistochemical analysis of 408 patients with the use of ten molecular markers. *J Thorac Cardiovasc Surg* 1999;117(4):736-43.
- Do H, Wong NC, Murone C, John T, Solomon B, Mitchell PL, *et al.* A critical re-assessment of DNA repair gene promoter methylation in non-small cell lung carcinoma. *Sci Rep* 2014;4:4186 doi 10.1038/srep04186.
- Eberhardt W, Pottgen C, Stuschke M. Chemoradiation paradigm for the treatment of lung cancer. *Nat Clin Pract Oncol* 2006;3(4):188-99 doi 10.1038/ncponc0461.
- Gaymes TJ, Shall S, MacPherson LJ, Twine NA, Lea NC, Farzaneh F, *et al.* Inhibitors of poly ADP-ribose polymerase (PARP) induce apoptosis of myeloid leukemic cells: potential for therapy of myeloid leukemia and myelodysplastic syndromes. *Haematologica* 2009;94(5):638-46 doi 10.3324/haematol.2008.001933.

- Goldstraw P, Crowley J, Chansky K, Giroux DJ, Groome PA, Rami-Porta R, *et al.* The IASLC Lung Cancer Staging Project: proposals for the revision of the TNM stage groupings in the forthcoming (seventh) edition of the TNM Classification of malignant tumours. *J Thorac Oncol* 2007;2(8):706-14 doi 10.1097/JTO.0b013e31812f3c1a.
- Helleday T. The underlying mechanism for the PARP and BRCA synthetic lethality: clearing up the misunderstandings. *Mol Oncol* 2011;5(4):387-93 doi 10.1016/j.molonc.2011.07.001.
- Hopwood P, Stephens RJ. Symptoms at presentation for treatment in patients with lung cancer: implications for the evaluation of palliative treatment. The Medical Research Council (MRC) Lung Cancer Working Party. *Br J Cancer* 1995;71(3):633-6.
- Issa JP, Garcia-Manero G, Giles FJ, Mannari R, Thomas D, Faderl S, *et al.* Phase 1 study of low-dose prolonged exposure schedules of the hypomethylating agent 5-aza-2'-deoxycytidine (decitabine) in hematopoietic malignancies. *Blood* 2004;103(5):1635-40 doi 10.1182/blood-2003-03-0687.
- Jabbari K, Bernardi G. Cytosine methylation and CpG, TpG (CpA) and TpA frequencies. *Gene* 2004;333:143-9 doi 10.1016/j.gene.2004.02.043.
- Jamal-Hanjani M, Wilson GA, McGranahan N, Birkbak NJ, Watkins TBK, Veeriah S, *et al.* Tracking the Evolution of Non-Small-Cell Lung Cancer. *N Engl J Med* 2017 doi 10.1056/NEJMoa1616288.
- Javle M, Curtin NJ. The role of PARP in DNA repair and its therapeutic exploitation. *Br J Cancer* 2011;105(8):1114-22 doi 10.1038/bjc.2011.382.
- Kedar PS, Stefanick DF, Horton JK, Wilson SH. Increased PARP-1 association with DNA in alkylation damaged, PARP-inhibited mouse fibroblasts. *Mol Cancer Res* 2012;10(3):360-8 doi 10.1158/1541-7786.MCR-11-0477.
- Kenfield SA, Wei EK, Stampfer MJ, Rosner BA, Colditz GA. Comparison of aspects of smoking among the four histological types of lung cancer. *Tob Control* 2008;17(3):198-204 doi 10.1136/tc.2007.022582.
- Kim G, Ison G, McKee AE, Zhang H, Tang S, Gwise T, *et al.* FDA Approval Summary: Olaparib Monotherapy in Patients with Deleterious Germline BRCA-Mutated Advanced Ovarian Cancer Treated with Three or More Lines of Chemotherapy. *Clin Cancer Res* 2015;21(19):4257-61
- Kim HJ, Kim JH, Chie EK, Young PD, Kim IA, Kim IH. DNMT (DNA methyltransferase) inhibitors radiosensitize human cancer cells by suppressing DNA repair activity. *Radiat Oncol* 2012;7:39 doi 10.1186/1748-717X-7-39.

- Kim TH, Cho KH, Pyo HR, Lee JS, Zo JI, Lee DH, *et al.* Dose-volumetric parameters for predicting severe radiation pneumonitis after three-dimensional conformal radiation therapy for lung cancer. *Radiology* 2005;235(1):208-15 doi 10.1148/radiol.2351040248.
- Kong FM, Zhao J, Wang J, Faivre-Finn C. Radiation dose effect in locally advanced non-small cell lung cancer. *J Thorac Dis* 2014;6(4):336-47 doi 10.3978/j.issn.2072-1439.2014.01.23.
- Lai TH, Ewald B, Zecevic A, Liu C, Sulda M, Papaioannou D, *et al.* HDAC Inhibition Induces MicroRNA-182, which Targets RAD51 and Impairs HR Repair to Sensitize Cells to Sapacitabine in Acute Myelogenous Leukemia. *Clin Cancer Res* 2016;22(14):3537-49 doi 10.1158/1078-0432.CCR-15-1063.
- Langelier MF, Planck JL, Roy S, Pascal JM. Structural basis for DNA damage-dependent poly(ADP-ribosylation) by human PARP-1. *Science* 2012;336(6082):728-32 doi 10.1126/science.1216338.
- Leung AW, de Silva T, Bally MB, Lockwood WW. Synthetic lethality in lung cancer and translation to clinical therapies. *Mol Cancer* 2016;15(1):61 doi 10.1186/s12943-016-0546-y.
- Lupo B, Trusolino L. Inhibition of poly(ADP-ribosylation) in cancer: old and new paradigms revisited. *Biochim Biophys Acta* 2014;1846(1):201-15 doi 10.1016/j.bbcan.2014.07.004.
- Lynch T, Kim E. Optimizing chemotherapy and targeted agent combinations in NSCLC. *Lung Cancer* 2005;50S2:S25-S32.
- Mahmood S, Bilal H, Faivre-Finn C, Shah R. Is stereotactic ablative radiotherapy equivalent to sublobar resection in high-risk surgical patients with stage I non-small-cell lung cancer? *Interact Cardiovasc Thorac Surg* 2013;17(5):845-53 doi 10.1093/icvts/ivt262.
- Murai J, Huang SY, Das BB, Renaud A, Zhang Y, Doroshow JH, *et al.* Trapping of PARP1 and PARP2 by Clinical PARP Inhibitors. *Cancer Res* 2012;72(21):5588-99 doi 10.1158/0008-5472.CAN-12-2753.
- Murai J, Huang SY, Renaud A, Zhang Y, Ji J, Takeda S, *et al.* Stereospecific PARP trapping by BMN 673 and comparison with olaparib and rucaparib. *Mol Cancer Ther* 2014;13(2):433-43 doi 10.1158/1535-7163.MCT-13-0803.
- Muvarak NE, *et al.* Enhancing the Cytotoxic Effects of PARP Inhibitors by DNA Demethylating Agents - A Potential Therapy for Cancer. In: FV R, editor. Volume 15. *Cancer Cell* 2016.

- Nguyen KS, Neal JW. First-line treatment of EGFR-mutant non-small-cell lung cancer: the role of erlotinib and other tyrosine kinase inhibitors. *Biologics* 2012;6:337-45 doi 10.2147/BTT.S26558.
- Nijman SM. Synthetic lethality: general principles, utility and detection using genetic screens in human cells. *FEBS Lett* 2011;585(1):1-6 doi 10.1016/j.febslet.2010.11.024.
- Paez JG, Janne PA, Lee JC, Tracy S, Greulich H, Gabriel S, *et al.* EGFR mutations in lung cancer: correlation with clinical response to gefitinib therapy. *Science* 2004;304(5676):1497-500 doi 10.1126/science.1099314.
- Palma DA, Senan S. Improving outcomes for high-risk patients with early-stage non-small-cell lung cancer: insights from population-based data and the role of stereotactic ablative radiotherapy. *Clin Lung Cancer* 2013;14(1):1-5 doi 10.1016/j.clcc.2012.06.005.
- Pisters KM, Evans WK, Azzoli CG, Kris MG, Smith CA, Desch CE, *et al.* Cancer Care Ontario and American Society of Clinical Oncology adjuvant chemotherapy and adjuvant radiation therapy for stages I-IIIa resectable non small-cell lung cancer guideline. *J Clin Oncol* 2007;25(34):5506-18 doi 10.1200/JCO.2007.14.1226.
- Ramroth J, Cutter DJ, Darby SC, Higgins GS, McGale P, Partridge M, *et al.* Dose and Fractionation in Radiation Therapy of Curative Intent for Non-Small Cell Lung Cancer: Meta-Analysis of Randomized Trials. *Int J Radiat Oncol Biol Phys* 2016;96(4):736-47 doi 10.1016/j.ijrobp.2016.07.022.
- Reale A, Matteis GD, Galleazzi G, Zampieri M, Caiafa P. Modulation of DNMT1 activity by ADP-ribose polymers. *Oncogene* 2005;24(1):13-9.
- Rigi-Ladiz MA, Kordi-Tamandani DM, Torkamanzehe A. Analysis of hypermethylation and expression profiles of APC and ATM genes in patients with oral squamous cell carcinoma. *Clin Epigenetics* 2011;3:6 doi 10.1186/1868-7083-3-6.
- Robertson KD, Uzvolgyi E, Liang G, Talmadge C, Sumegi J, Gonzales FA, *et al.* The human DNA methyltransferases (DNMTs) 1, 3a and 3b: coordinate mRNA expression in normal tissues and overexpression in tumors. *Nucleic Acids Res* 1999;27(11):2291-8.
- Rodrigues G, Lock M, D'Souza D, Yu E, Van Dyk J. Prediction of radiation pneumonitis by dose - volume histogram parameters in lung cancer--a systematic review. *Radiother Oncol* 2004;71(2):127-38 doi 10.1016/j.radonc.2004.02.015.
- Roots R, Kraft G, Gosschalk E. The formation of radiation-induced DNA breaks: the ratio of double-strand breaks to single-strand breaks. *Int J Radiat Oncol Biol Phys* 1985;11(2):259-65.

- Rose-James A, Tt S. Molecular Markers with Predictive and Prognostic Relevance in Lung Cancer. *Lung Cancer Int* 2012;2012:729532 doi 10.1155/2012/729532.
- Santivasi WL, Xia F. Ionizing radiation-induced DNA damage, response, and repair. *Antioxid Redox Signal* 2014;21(2):251-9 doi 10.1089/ars.2013.5668.
- Sedletska Y, Radicella JP, Sage E. Replication fork collapse is a major cause of the high mutation frequency at three-base lesion clusters. *Nucleic Acids Res* 2013;41(20):9339-48 doi 10.1093/nar/gkt731.
- Shen Y, Aoyagi-Scharber M, Wang B. Trapping Poly(ADP-Ribose) Polymerase. *J Pharmacol Exp Ther* 2015;353(3):446-57 doi 10.1124/jpet.114.222448.
- Siegel RL, Miller KD, Jemal A. Cancer Statistics, 2017. *CA Cancer J Clin* 2017;67(1):7-30 doi 10.3322/caac.21387.
- Tsai HC, Li H, Van Neste L, Cai Y, Robert C, Rassool FV, *et al.* Transient low doses of DNA-demethylating agents exert durable antitumor effects on hematological and epithelial tumor cells. *Cancer Cell* 2012;21(3):430-46 doi 10.1016/j.ccr.2011.12.029.
- Verhagen CV, de Haan R, Hageman F, Oostendorp TP, Carli AL, O'Connor MJ, *et al.* Extent of radiosensitization by the PARP inhibitor olaparib depends on its dose, the radiation dose and the integrity of the homologous recombination pathway of tumor cells. *Radiother Oncol* 2015;116(3):358-65 doi 10.1016/j.radonc.2015.03.028.
- Wang B, Chu D, Feng Y, Shen Y, Aoyagi-Scharber M, Post LE. Discovery and Characterization of (8S,9R)-5-Fluoro-8-(4-fluorophenyl)-9-(1-methyl-1H-1,2,4-triazol-5-yl)-2,7,8,9-tetrahydro-3H-pyrido[4,3,2-de]phthalazin-3-one (BMN 673, Talazoparib), a Novel, Highly Potent, and Orally Efficacious Poly(ADP-ribose) Polymerase-1/2 Inhibitor, as an Anticancer Agent. *J Med Chem* 2016.
- Wang M, Wu W, Rosidi B, Zhang L, Wang H, Iliakis G. PARP-1 and Ku compete for repair of DNA double strand breaks by distinct NHEJ pathways. *Nucleic Acids Res* 2006;34(21):6170-82 doi 10.1093/nar/gkl840.
- Wang X, Weaver DT. The ups and downs of DNA repair biomarkers for PARP inhibitor therapies. *Am J Cancer Res* 2011;1(3):301-27.
- Woodard GA, Jones KD, Jablons DM. Lung Cancer Staging and Prognosis. *Cancer Treat Res* 2016;170:47-75 doi 10.1007/978-3-319-40389-2\_3.